



# Fate of recently assimilated carbon in the soil–plant system of *Vaccinium vitis-idaea* and its response to warming in a 2.5-year translocation experiment

Valentin B. Kurbel · Outi-Maaria Sietiö · Kristiina Karhu · Andrei Rodionov · Sari Timonen · Thomas Ohnemus · Eva Lehndorff · Johanna Pausch · Nele Meyer

Received: 17 December 2024 / Accepted: 11 October 2025 / Published online: 2 December 2025  
© The Author(s) 2025

## Abstract

**Background and aims** Shrubs like *Vaccinium vitis-idaea* substantially contribute to forest carbon (C) sequestration. Therefore, understanding their allocation patterns under climate change is crucial. We conducted a translocation experiment with  $^{13}\text{CO}_2$  pulse-labelling to test if (I) belowground pools accumulate total and recently assimilated C, (II) within fine roots, assimilated C is preferentially allocated to root tips and mycorrhized cells and (III), whether warming alters C allocation patterns.

**Methods** We translocated soil cores with *V. vitis-idaea* from North- to South-Finland (+3.7 °C mean

temperature). After 2.5 years, we excavated and pulse-labelled them with  $^{13}\text{CO}_2$ , tracing the  $^{13}\text{C}$  in plant, soil, and respiration. We used laser-ablation isotope ratio mass spectrometry to examine  $^{13}\text{C}$  distribution in fine roots.

**Results** Roots represented the largest plant C pool (north:  $49.69 \pm 9.73\%$ , translocated:  $43.92 \pm 6.59\%$  of plant C stock). A substantial amount of recently assimilated  $^{13}\text{C}$  was recovered belowground (roots+soil, north:  $15.59 \pm 5.77\%$ , translocated:  $39.21 \pm 29.32\%$ ) 8 days after labelling. Most assimilated C was respired (north:  $63.3 \pm 5.9\%$ , translocated:  $44.1 \pm 3.2\%$ ) or recovered in leaves (north:  $17.9 \pm 5.92\%$ , translocated:  $19.2 \pm 3.19\%$ ). Within fine roots,  $^{13}\text{C}$  content tended to be higher at root tips, while mycorrhizal infection had

Responsible Editor: Yolima Carrillo.

V. B. Kurbel (✉) · T. Ohnemus · J. Pausch  
Agroecology, Bayreuth Center of Ecology  
and Environmental Research (BayCEER), University  
of Bayreuth, Bayreuth, Germany  
e-mail: valentin.kurbel@uni-bayreuth.de

V. B. Kurbel · A. Rodionov · E. Lehndorff · N. Meyer  
Soil Ecology, Bayreuth Center of Ecology  
and Environmental Research (BayCEER), University  
of Bayreuth, Bayreuth, Germany

O.-M. Sietiö  
HAMK Bio Research Unit, Häme University of Applied  
Research, Hämeenlinna, Finland

K. Karhu  
Department of Forest Sciences, University of Helsinki,  
Helsinki, Finland

K. Karhu  
Helsinki Institute of Life Sciences (HiLIFE), University  
of Helsinki, Helsinki, Finland

S. Timonen  
Department of Microbiology, University of Helsinki,  
Helsinki, Finland

T. Ohnemus  
Department of Monitoring- and Exploration Technologies,  
Helmholtz Centre for Environmental Research – UFZ,  
Leipzig, Germany

N. Meyer  
Institute of Physical Geography, Goethe-University  
Frankfurt, Frankfurt, Germany

no effect. Warming tended to increase C allocation to the shoot and significantly decreased  $^{13}\text{C}$  in the microbial biomass in the mineral soil.

**Conclusion** *V. vitis-idaea* allocates a large portion of assimilates belowground, but 2.5 years of warming only marginally change C allocation patterns. Accelerated soil microbial processes after translocation may increase plant N availability, potentially affecting C allocation over longer time spans.

**Keywords** Climate warming · *Ericaceae* · Stable isotopes · Laser ablation mass spectrometry · Carbon allocation

### Abbreviations

|         |  |
|---------|--|
| C       | Carbon   |
| CFE     | Chloroform-Fumigation-Extraction               |
| ErM     | Ericoid Mycorrhiza                             |
| f       | Fumigated                                      |
| LA-IRMS | Laser-Ablation Isotope Ratio Mass Spectrometry |
| MBC     | Microbial Biomass Carbon                       |
| N       | Nitrogen                                       |
| nf      | Non-fumigated                                  |
| OLS     | Ordinary Least Square                          |
| SOM     | Soil Organic Matter                            |
| TOC     | Total Organic Carbon                           |
| VPDB    | Vienna Pee Dee Belemnite                       |

### Introduction

Boreal forests are recognized as significant global reservoirs of carbon (C), with estimations ranging from 367.3 to 1715.8 Pg (Bradshaw and Warkentin 2015). This implies the need to understand C-related processes in these ecosystems to minimize C losses as a mitigation strategy of global change. The soil of the boreal forest, which represents the biggest C storage in these systems (Bradshaw and Warkentin 2015), is densely covered with dwarf shrubs belonging to the *Ericaceae* family, including *Vaccinium vitis-idaea* (L). The contribution of these shrubs to the boreal forest net primary production ranges between 10 and 20% (Bergeron et al. 2009; Ilvesniemi et al. 2009; Kulmala et al. 2011; Kolari et al. 2006; Swanson and Flanagan 2001). Further, these shrubs drive autotrophic respiration (Mielke et al. 2022) and affect soil C and nitrogen (N) dynamics (Clemmensen et al.

2015; Sietiö et al. 2018; Ward et al. 2022). *Vaccinium* species are adapted to the harsh conditions of boreal forests of high-latitude ecosystems, where nutrients, especially N, are often limiting plant growth (Lupi 2013, Högberg et al. 2017).

To cope with these conditions, *Vaccinium* species usually live in close symbiotic associations with ericoid mycorrhizal (ErM) fungi. The fungi partly form chemically stable biomass with a high melanin content as a mechanism of stress adaptation. In general, the C in mycorrhizal mycelium was proposed to be a major pool retaining C in the soil (Hawkins et al. 2023), which could be especially true for ErM fungi given that the high melanin content increases its turnover time in the soil (Clemmensen et al. 2015). To cope with nutrient deficiencies in the boreal system, plants invest a large portion of assimilated C in nutrient acquisition. For example, for *V. myrtillus* and *V. vitis-idaea*, it was shown that roughly 50% of the biomass is accumulating belowground (Kulmala et al. 2018). Similar results were also obtained by isotope labelling of shrubs in other ecosystems (Gavrichkova et al. 2017; Olsrud and Christensen 2011), indicating that a large portion of C is usually invested in the root system to increase the foraging capacity for nutrients. Furthermore, based on respiration measurements, Kulmala et al. (2018) suggested that a large fraction of recently assimilated C is exuded into the soil by *Vaccinium* species in boreal forests. This can fuel symbiotic interactions, such as the ErM association, to further increase the nutrient supply to the plant (Smith and Read 2010; van der Heijden et al. 2008). Based on  $^{14}\text{CO}_2$  labelling of grasses, high C release into the soil of up to 80% was shown (Warembourg et al. 1990; Kuzyakov 2001), but similarly clear evidence for shrubs in boreal forests is still lacking. Despite the crucial role of belowground C allocation patterns for soil C sequestration, only few studies investigated belowground C transfer of *Vaccinium* species (Anadon-Rossel et al. 2017; Kulmala et al. 2018). However, none of these studies were conducted in the boreal system, bearing the danger of missing out a crucial contributor to forest C storage.

As plant and microbial processes are usually temperature driven, global change and associated temperature increases can be expected to affect C partitioning in the plant-soil systems of boreal shrubs. Warming may increase respiration processes and thus affect  $\text{CO}_2$  losses (Melillo et al. 2002; Bekku et al. 2003), and

higher temperatures may lead to better plant performance, resulting in altered CO<sub>2</sub> uptake (Forkel et al. 2016). Moreover, as the microbial processes in the soil are accelerated, more soil organic matter (SOM) is mineralized, and more nutrients are mobilized by the soil microbiome (Bai et al. 2013; Schmidt et al. 2002). As a result, plant nutrient limitation may decrease, leading to a less C allocation to roots, soil, and soil microorganisms due to warming, which could influence soil C sequestration. Indeed, across 3000 alpine plots, many plants shifted their biomass above ground under global warming (Yun et al. 2024). However, such an effect of warming seems to be context- and species specific (Yun et al. 2024) and has not yet been studied specifically for boreal shrubs like *V. vitis-idaea*, leaving a potential effect of climate change on boreal forest C sequestration understudied.

Most studies that investigated the effect of warming on processes in soil-shrub systems relied on artificial in-situ warming of the soil (Dawes et al. 2011) or the atmosphere (Gavrichkova et al. 2017). However, an artificial warming approach bears several risks: Edge effects are common and the sudden increase in temperature alone can unnaturally affect several environmental parameters of the surrounding, such as moisture and gas concentrations. By translocating plants along a climate gradient, in contrast, the samples get exposed to a realistic change in conditions such as higher temperature on the plot scale (Backhaus et al. 2014). In this study, we therefore simulated climate warming with a translocation approach in a boreal ecosystem to close the existing knowledge gaps relevant for forest C sequestration – i.e. the missing information about C allocation patterns in *V. vitis-idaea* and its response to warming. Specifically, we hypothesized:

- (I) Irrespective of temperature, *V. vitis-idaea* invests a high proportion of assimilates into nutrient acquisition. Therefore, roots represent the largest plant biomass C pool, and a larger proportion of recently assimilated C is allocated belowground to the roots, the surrounding soil, and the soil microbial biomass in comparison with aboveground plant biomass.
- (II) Within fine roots, a larger proportion of recently assimilated C is transferred to the root tips and to cells colonized by mycorrhizal fungi than to other root parts, as *V. vitis-idaea* - irre-

spectively of temperature - especially invests into nutrient acquisition strategies.

- (III) As SOM decomposition and the resultant nutrient supply increase with rising temperatures, C allocation for nutrient acquisition shifts, leading to reduced C transfer to roots, soil, and microbial biomass.

To address these hypotheses, we conducted a translocation experiment exposing intact plant-soil systems with *V. vitis-idaea* to an increase of 3.7 °C in the mean temperature. After 2.5 years, we combined <sup>13</sup>C<sub>2</sub> pulse labelling with subsequent extraction of soil microbial biomass C, root staining to visualize ErM colonization, and small scale <sup>13</sup>C tracing in fine roots with Laser Ablation-Isotope Ratio Mass Spectrometry (LA-IRMS) to understand C allocation patterns in boreal dwarf shrubs and its surrounding soil and its response to global warming.

## Material and methods

### Translocation

To conduct the translocation, the following two sites were selected: Kivalo in North-Finland (Lat: 66°21'37.504", Lon: 26°43'35.382") and Tammela in South-Finland (Lat: 60°36'54.648", Lon: 23°50'17.847", Fig. 1). These sites were chosen to achieve a temperature increase predicted for Finland by the end of the century, which is estimated – depending on the scenario – around 4 °C (moderate emission scenario, SSP2-4.5, Ruosteenoja & Jylhä, 2021). Translocation between these two sites, which are in vicinity of long-term monitored undisturbed forest sites (Merilä et al. 2024) increased the mean temperature by 3.7 °C, from 2.17 °C to 5.94 °C (Table 1, Finnish Meteorological Institute 2025). Besides the temperature, general properties were comparable between the two sites: both were coniferous forests on podzols dominated by *Pinus sylvestris*, with the understory vegetation being dominated by *Vaccinium* sp. (Fig. 1, for further details on the sites, see Merilä et al. (2024) and Merilä et al. (2014)). In October 2019, four intact soil cores (PVC tubes, 10 cm diameter, 26 cm length) were taken from Kivalo and intactly buried in the soil in Tammela at the same depth they originated from. With these core dimensions, the typical root depth of *Vaccinium* sp. was fully included (Ding et al. 2019).

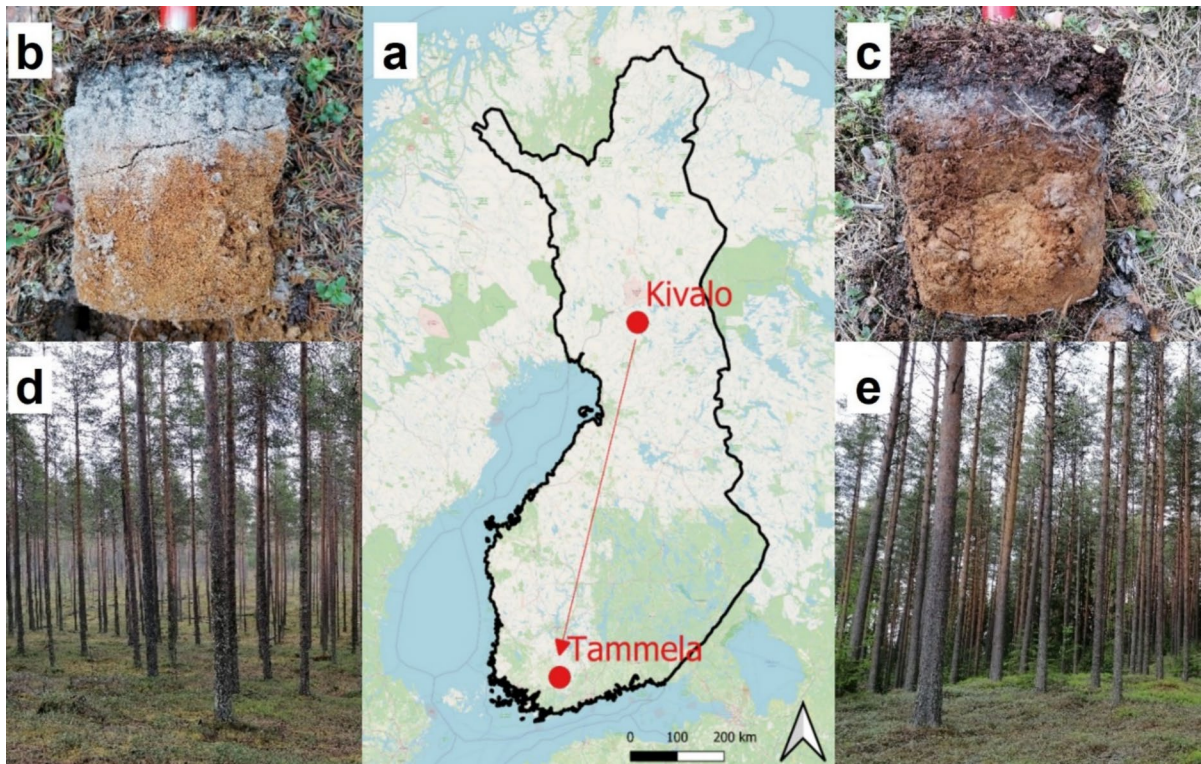


**Fig. 1** Field sites of this study: To study the effect of warming on carbon allocation in the plant-soil system of *V. vitis-idaea*, intact soil cores were taken from North-Finland (Kivalo, b, d)

and translocated to South-Finland (Tammela, c, e), where they were buried in the soil. This exposed them to an increase in 3.7 °C in mean temperature (a, map created with ArcGIS)

**Table 1** Weather data for the sites used in this study. Samples were translocated from Kivalo to Tammela to simulate warming. Data was obtained for the years 2020 and 2021 from

nearby weather stations (Rovaniemi Airport near Kivalo and Somero Salkola near Tammela, Finnish Meteorological Institute 2025)

|                 | Average daily temperature (°C) | Average Max. daily temp. (°C) | Highest Max. daily temp. (°C) | Average Min. daily temp. (°C) | Lowest Min. daily temp. (°C) | Precipitation (mm/year) |
|-----------------|--------------------------------|-------------------------------|-------------------------------|-------------------------------|------------------------------|-------------------------|
| Kivalo (North)  | 2.2                            | 5.67                          | 30                            | −1.29                         | −28.7                        | 656.75                  |
| Tammela (South) | 5.9                            | 9.45                          | 31.4                          | 2.55                          | −23.6                        | 708.9                   |

Each core contained at least one individual shoot of *V. vitis-idaea*. The bottom of the cores was closed with a mesh to prevent root ingrowth from the surrounding soil while ensuring vertical water flow. However, lateral water flow is hampered by the PVC tubes. Yet, to ensure comparability of the translocated cores, four cores were also translocated on-site in Kivalo. All cores were excavated again in June 2022, i.e. 2.5 years after translocation, and transferred to a climate chamber with controlled temperature and light conditions (22 °C and

a light:dark-cycle (18:6), lamps with 15.1 W, 3000 or 4000 K, and 2250 lm). Controlled temperature conditions were chosen for this experiment instead of ambient temperature because we aimed at exploring how adaptation to 2.5 years of warming affected C assimilation and sequestration patterns rather than the immediate effect of higher temperatures. These chosen temperature conditions in the chamber approximate high summer temperatures on the selected field sites (Table 1), ensuring high assimilation rates, but still represent realistic

temperature conditions. The used light intensity is typical for light forests (Coetzee et al. 2024). Four additional samples with *V. vitis-idaea* were taken in Kivalo in 10 cm diameter cores and stored at  $-20^{\circ}\text{C}$ . These samples were later used as controls for natural abundance isotope measurements. Similarly, three natural abundance cores were taken in Tammela which were later used for the LA-IRMS measurement.

#### Pulse labelling and measurement of $^{13}\text{C}$ respiration

Before isotope labelling was conducted, the plants were kept in the climate chamber for one day to allow them to acclimate to the new conditions and to alleviate sampling-induced stress. The duration of only one day was chosen to ensure that transplantation effects are not masked by the temperature in the climate chamber. Still, minor effects introduced by the climate chamber cannot be excluded. The eight cores (four cores translocated from North to South and four cores translocated outside in the North) were transferred into a transparent gas-tight labelling box (volume:  $0.17\text{ m}^3$ ) within the climate chamber. A bottle containing a mixture of 25 mL distilled water, 0.3 mL 1 M sodium hydroxide, and 2 g of 99%  $^{13}\text{C}$ -enriched sodium carbonate was connected to the box via a tube. Divided by the number of plants in

the labelling box (in total 15 plants, yet only 8 used in this study), this resulted in an amount of 17.35 mg  $^{13}\text{C}$  added per plant (hereafter: added tracer, Table 2). To start the labelling, 50 mL of sulfuric acid (5 M) was added to the solution dropwise within 20 min, releasing  $^{13}\text{CO}_2$  into the box. Theoretically, this resulted in an increase of 2700 ppm  $^{13}\text{CO}_2$ . A fan inside the box ensured mixing of the  $^{13}\text{CO}_2$  within the box. The cores were then removed from the labelling box and remained in the climate chamber under unlabelled atmospheric conditions for eight days during which the cores were regularly watered.

To measure  $^{13}\text{CO}_2$  respiration, the cores were transferred into a gastight and dark container for one hour. The gas containers had a volume of around  $0.02\text{ m}^3$  and gas mixing was ensured by the installation of a fan inside the container. Respiration measurements were conducted daily starting one day after  $^{13}\text{CO}_2$  labelling and once before labelling as control for the natural abundance isotope signature of  $\text{CO}_2$ . During the one hour of incubation, air from each container was sampled four times manually with a syringe through a septum and injected into an EGM-4 gas analyser (Environmental Gas Monitor, PP Systems, Amesbury, USA) to measure the  $\text{CO}_2$  concentration. The concentration values were transferred into masses of C (Eq. 1), before a slope was calculated to obtain the C efflux per hour.

$$m(\text{C})[\text{mgC}] = \frac{c(\text{CO}_2)[\text{ppm}] * 10^{-6} * p[\text{Pa}] * V[\text{cm}^3] * 12[\text{g} * \text{mol}^{-1}] * 1000}{T[\text{K}] * R[\text{J} * \text{mol}^{-1} * \text{K}^{-1}]} \quad (1)$$

Within the one hour of incubation, 8 mL air were sampled at the first and the last gas sampling for  $^{13}\text{C}$ -isotope analyses of  $\text{CO}_2$ . The gas samples were transferred into  $\text{N}_2$  containing exetainers (original volume: 12 mL). To create an overpressure in the exetainer, only 6 ml of the  $\text{N}_2$  in the exetainer were removed before the sample was injected. The  $^{13}\text{C}$  content of the  $\text{CO}_2$  was determined with a GC (column: CP-PoraPLOT Q, Agilent, Santa Clara, USA) coupled with an IRMS (MAT 253, Thermo Finnigan, San Jose, USA). Vienna-Pee Dee Belemnite (VPDB;  $R=0.0111802$ ) was used as standard for C. To purify the  $\delta^{13}\text{C}$  value of  $\text{CO}_2$  released from the plant-soil cores for atmospheric admixture, i.e. atmospheric  $\text{CO}_2$  in the gastight container, Miller/Tans plots were applied using an ordinary least square (OLS) regression (Miller and Tans 2003). For each treatment and

day, the product of the isotopic composition of  $\text{CO}_2$  (‰) and its C concentration (ppm) from the eight daily measurements across four cores was plotted against the C concentration (ppm). The slope of the OLS regression line equals the integrated  $\delta^{13}\text{C}$  values of  $\text{CO}_2$  released from the plant-soil system without atmospheric  $\text{CO}_2$ . Thus, this value summarizes all four cores per treatment, potentially limiting statistical interference. As the natural abundance gas measurements that were conducted prior to labelling were contaminated with  $^{13}\text{C}$  for the northern samples, both treatments were compared to the  $^{13}\text{C}$  natural abundance of the translocated samples (atom%) to estimate  $^{13}\text{C}$  excess. Based on the  $\text{CO}_2$  flux per measurement and treatment and the corresponding atom% values of  $^{13}\text{C}$  in  $\text{CO}_2$ , the total  $^{13}\text{C}$  respired per hour was calculated. To quantify the cumulative  $^{13}\text{CO}_2$

efflux over the eight days, we fitted an exponential decay function (Eq. 2) using nonlinear least squares regression with R (R Core Team 2023). Next, we scaled the efflux per hour to daily efflux leading to the resulting integral representing the cumulative efflux of  $^{13}\text{CO}_2$  over the measuring period.

$$F(t) = F(0) * e^{-k*t} \quad (2)$$

Eight days after pulse labelling the cores were frozen at  $-20^\circ\text{C}$  until further processing.

### Destructive sampling of soil cores

For further analysis, the labeled and unlabeled control cores were thawed at room temperature and subsequently divided into shoot, leaves, roots, mineral soil, organic layer, and rhizosphere. The soil that was still attached to the roots after shaking three times was defined as rhizosphere and collected by washing and subsequent freeze-drying. The soil was sieved (5 mm) and dried for six days at  $40^\circ\text{C}$ . After root washing, few young root parts – determined visually as thin, bright roots in contrast to clearly woody parts of the root system – were collected from each plant and stored in distilled water at  $-20^\circ\text{C}$  to determine mycorrhizal colonization and respective  $^{13}\text{C}$  accumulation. Afterwards, all plant parts were dried for six days at  $40^\circ\text{C}$ .

### Isotopic analysis in soil, plant, and microbial biomass

To analyze the C content and  $^{13}\text{C}$  in soil and plant, the dried samples were milled (2 min,  $25\text{ s}^{-1}$ , MM 400, Retsch, Haan, Germany), whereby leaves, shoot, and roots were first frozen with liquid  $\text{N}_2$  to facilitate breaking of the material and obtaining a homogenous sample for  $^{13}\text{C}$  analysis. The C content and  $^{13}\text{C}$  were analyzed with an EA (Carlo Erba NC 2500, Milan, Italy) coupled with an IRMS (Delta plus) via the ConFlo III interface (both Thermo Fisher, Bremen, Germany). VPDB (R=0.0111802) was used as standard, against which the IRMS was calibrated with three different standards (CH3, CH6, CH7, all International Atomic Energy Agency, Vienna, Austria). To proceed, a calculation was performed to estimate which percentage of the assimilated C was allocated to the different pools. The  $^{13}\text{C}$  distributed to individual pools was calculated by multiplying the excess atom% (calculated by subtracting the atom% of the sample from the atom% of the northern natural abundance control) of  $^{13}\text{C}$  with the C content of the respective pools and referring it to the total  $^{13}\text{C}$  content (Eq. 3). The latter refers to the sum of the  $^{13}\text{C}$  content in the soil pools and the plant parts of the respective samples as well as the respiration value of the respective treatment (north vs. translocated). Thus, the total  $^{13}\text{C}$  recovered is different for all samples and the  $^{13}\text{C}$  distribution values only allow for relative comparison of allocation patterns.

$$^{13}\text{Cdistribution}[\%] = C[\text{mg} * \text{g}^{-1}] * \text{dryweight}[\text{g}] * ^{13}\text{C}[\text{atom}\%] * \frac{100}{\text{total}^{13}\text{C}[\text{recovered}[\text{mg}]]} \quad (3)$$

To measure the C content and  $^{13}\text{C}$  in microbial biomass C (MBC), a chloroform-fumigation-extraction (CFE) was conducted (Vance et al. 1987). From each soil core approximately 10 g fresh weight (FW) sieved mineral soil or 4 g FW organic layer were fumigated with chloroform in a vacuum desiccator for 24 h. Following that, the samples and the same set of control samples, which were not fumigated with chloroform, were extracted with 40 mL of 0.5 M  $\text{K}_2\text{SO}_4$ . Samples were shaken for 1 h (overhead shaker, 240 rpm), filtered (Rotilabo® folded filter, type 113P), and split into two parts. One part

was used for determination of the total organic C (TOC) in 5 mL of the filtrates diluted 1:1 with distilled water (multi N/C 2100S, Analytik Jena, Jena, Germany). The other part was freeze-dried (Alpha 1–4 LSCbasic, Martin Christ Gefriertrocknungsanlagen, Osterode am Harz, Germany) and the  $^{13}\text{C}$  content was analyzed as described before. From the TOC of the fumigated (f) and non-fumigated (nf) samples, MBC was calculated using Eqs. 4 and 5, where V is the volume of added  $\text{K}_2\text{SO}_4$ . A factor of 0.45 was used as the microbially bound C is typically underestimated by CFE (Jenkinson et al. 2004).

$$C_{\text{extracted}} [mg * g^{-1}DW] = \frac{TOC [mg * l^{-1}] * 2 * V [l]}{DW [g]} \quad (4)$$

$$MBC [mg * g^{-1}DW] = \frac{C_f [mg * g^{-1}DW] - C_n [mg * g^{-1}DW]}{0.45} \quad (5)$$

$$\delta^{13}C_{MBC} [‰] = \frac{\delta^{13}C_f [‰] * C_f [\mu g * g^{-1}DW] - \delta^{13}C_{nf} [‰] * C_{nf} [\mu g * g^{-1}DW]}{C_f [\mu g * g^{-1}DW] - C_{nf} [\mu g * g^{-1}DW]} \quad (6)$$

### Small-scale visualization of intraradical ErM structures and $^{13}C$ -distribution in roots

To identify intraradical structures of ErM fungi, fine roots were soaked overnight at 40 °C in a solution of lactic acid and glycerol (1:1) with 0.05 % trypan blue. The stained roots were then transferred to another solution of lactic acid and glycerol (1:1) without trypan blue for 30 min and roots were categorized under the microscope.

Four sets of samples were selected for LA-IRMS with two to three root samples each: 1) Labelled and stained roots to investigate the effect of mycorrhizal colonization on the  $^{13}C$ , 2) unlabelled and stained roots as corresponding control for natural abundance, 3) labelled and non-stained roots in order to investigate whether  $^{13}C$  accumulates especially in root tips without any possible effects of the root staining method, and 4) unlabelled and non-stained roots as corresponding control for effects of staining on the isotopic signature.

We used LA-IRMS to analyze the small-scale distribution of recently assimilated  $^{13}CO_2$  in the root system depending on the position (proximal root (i.e. not the root tip) vs. tip) and ErM colonization (Fig. 6, Appendix). As LA-IRMS is very laborious and expensive, the number of considered roots was quite small, not allowing to systematically investigate the effect of translocation. Hence, roots for LA-IRMS were selected independent of them originating from North- or south-Finland.

Roots were embedded in water glass (sodium silicate solution, reagent grade,  $Na_2O_7Si_3$ , PN:338,443, Sigma-Aldrich, St. Louis, MO, USA) within a PTFE plate with cylindrical cavities of 1.5 mm depths and a diameter of 0.5 cm (Vergara Sosa et al. 2021). The water glass with embedded roots was dried at 60 °C. Afterwards,

Ultimately, the  $\delta^{13}C$  of MBC was calculated with Eq. 6 (Murage and Voroney 2007) and the share of the total assimilated  $^{13}C$  that was recovered in the microbial biomass was calculated analogously to Eq. 3, whereby an average of three natural abundance controls was used from northern control cores.

samples were collected from the PTFE cavities. Embedded roots were visually inspected under a binocular and for each root, 7–45 spots of 20  $\mu m$  diameter were selected for LA-IRMS measurements. For stained roots, the selected spots covered the following classes: uninfected root tips, infected root tips, uninfected proximal root, and infected proximal root. For non-stained roots, the selected spots covered the classes root tip and proximal root. The number of spots per class was not always balanced due to missing classes on some roots or unbalanced coverage.

For LA-IRMS measurements, we used a Teledyne LSX-213G2+ solid state Nd:YAG laser system (Teledyne LSX-213G2+, CETAC, Omaha, NE, USA) coupled to a 900 °C combustion oven, followed by two cryo-traps and a nafion trap for water (modified PreCon system) and an IRMS DeltaVplus with a ConFlo IV interface (all from Thermo-Fisher Scientific, Waltham, MA, USA (Rodionov et al. 2019)).

The ablations were produced with burst count of 40 shots within a spot size of 20  $\mu m$  size and in 0.4 mL cell volume. Rodionov et al. (2019) demonstrated that this spot size ablates sufficient C, even from materials with much lower C content than that found in roots. Interferences by embedding in sodium silicate solution were checked by sampling in the cell of the LA-IRMS system together with acryl as reference material (Rodionov et al. 2019). As reference the in-house acryl standard was used (C content 60%; density 1.19 g  $cm^3$ ;  $\delta^{13}C_{Acryl} = -29.75 \pm 0.06$  ‰, relative to VPDB using EA-IRMS). The  $\delta^{13}C$  of the  $CO_2$  background in the sample cell was at  $10.8 \pm 0.4$  mV, the acryl reference was at  $-29.75 \pm 0.20$  ‰.

A blank correction (i.e. measurement without ablation; signal may originate from small amounts of  $CO_2$  already present in the cell or resulting from other tiny leakages in the system) for isotope ratio measurement with small

amounts of samples can be performed by regression or by subtraction (Werner and Brand 2001; Ohlsson 2013) and calculated as described by Werner et al. (1999) and Eq. 7, where A is the area of the  $m/z$  44 peak.

$$\delta^{13}C_{\text{sample}} [\text{‰}] = \frac{(\delta^{13}C_{\text{total}} [\text{‰}] * A_{\text{total}} - \delta^{13}C_{\text{blank}} [\text{‰}] * A_{\text{blank}})}{(A_{\text{total}} - A_{\text{blank}})} \quad (7)$$

### Statistical analysis and data visualization

R (R Core Team 2023) and Sigmaplot (Sigmaplot for Windows V15.0) were used for statistical analysis and data visualization, whereby in R, the packages ggplot2 (Wickham 2016), ggpattern (FC et al. 2025), and cowplot (Wilke 2024) were used for the creation of figures.

To compare two groups (translocated vs. non-translocated), a student's t-test was performed after testing for normal distribution and homogeneity of variances. For the non-parametric comparison of two levels within one factor, a Wilcoxon test was performed (to analyse  $^{13}\text{C}$  in the fine roots). For comparison of the two groups under different variables (e.g. translocated vs. non-translocated in different soil and plant pools), a two-way ANOVA was performed after analyzing the residuals of the ANOVA for normal distribution and the data for homogeneity of variances using the package car (Fox et al. 2012). In the case of homoscedastic or non-normally distributed residuals, an aligned rank transformed (ART) ANOVA was performed with the package ARTool (Kay et al. 2025; Wobbrock et al. 2011). TukeyHSD was used as posthoc test for the

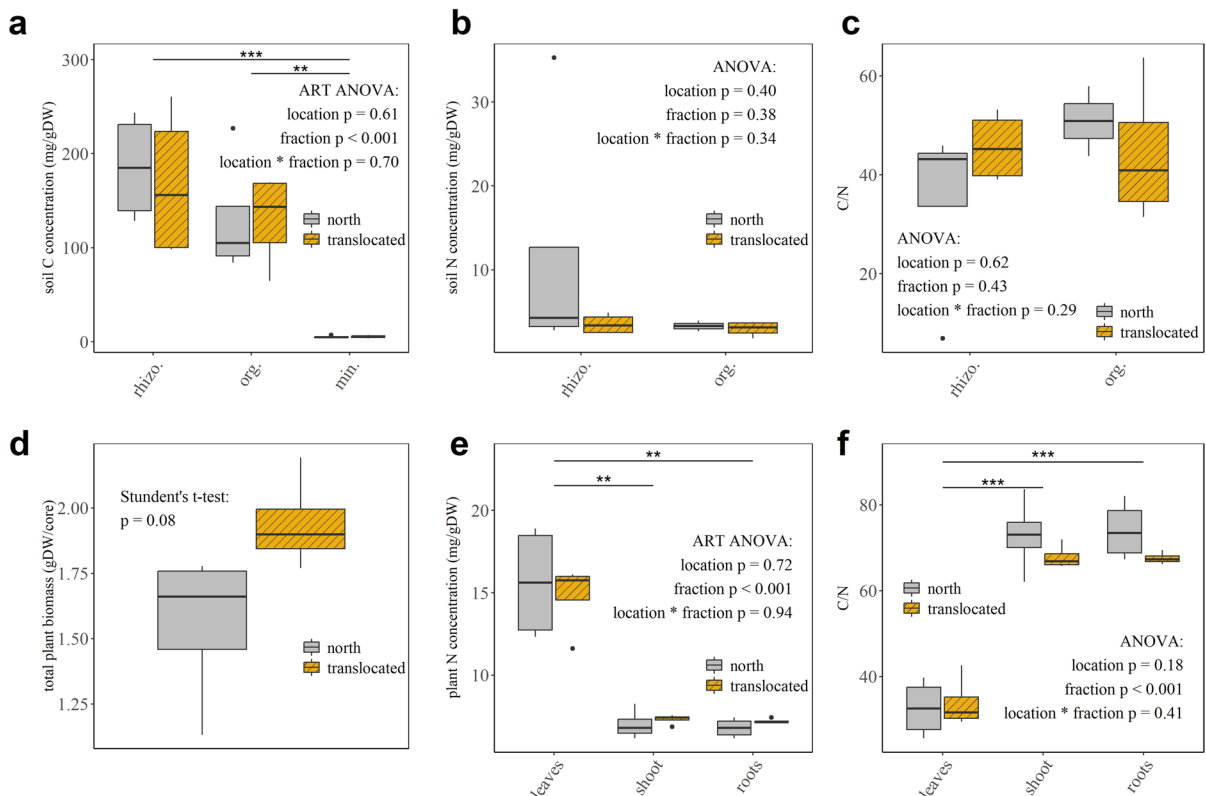


**Fig. 2** Soil and plant (*V. vitis-idaea*) carbon (C) and nitrogen (N) status: Soil C (**a**), soil N (**b**), and soil molar C/N ratio (**c**) of the rhizosphere (rhizos., i.e. soil attached to the roots), the organic layer (org.) and the mineral soil (min.) as well as the plant biomass (**d**), plant N (**e**) and plant molar C/N ratio (**f**) of the plant pools leaves, shoot, and roots of intact soil cores with *V. vitis-idaea* that were either translocated from north to south Finland (+3.7 °C mean temperature, yellow, stripes) or

translocated on site in north Finland (grey) and excavated after 2.5 years. Asterisks indicate significant differences ( $p = 0.05 < * < 0.01 < ** < 0.001 < ***$ ) tested with a two-way ANOVA with  $n = 4$  except of N and C/N in the org. layer ( $n = 2$ , due to results below limit of detection). ANOVA was followed by a TukeyHSD test as respective posthoc test. Mineral soil N was excluded due to results below limit of detection

ANOVA, while a posthoc test on estimated marginal means was performed after ART-ANOVA. The latter was performed with the emmeans package (Lenth 2025). To analyze the distribution of  $^{13}\text{C}$  in the fine-roots, a Kruskal–Wallis test was performed in R.

## Results

The C/N ratio of the soils was around 50 for both treatments (translocated and northern controls) in the rhizosphere and the organic layer (Fig. 2c). N was below detection limit in most mineral soil samples. In the rhizosphere, the N content showed a tendency to decrease with translocation (Fig. 2b), which was accompanied by a tendency of increasing C/N ratio (Fig. 2c). The translocation did not affect soil C contents in the rhizosphere (Fig. 2a), nor soil C and N contents in the organic layer (Fig. 2a, b). The dry weight of the plant biomass increased with translocation, yet not significantly (Fig. 2d). Irrespective of the translocation, total plant N and the C/N in the plant differed significantly between the plant pools with leaves showing higher N contents than the plant shoot and roots (Fig. 2e). Translocation tended to decrease the C/N ratio of the plant shoot and roots, although this decrease was not significant (Fig. 2f).

Total plant C tended to be higher in the translocated samples than the northern controls (Fig. 3a). The C distributed unequally between the different plant pools: Roots had the highest relative portion of plant C, followed by the shoot and the leaves. Although not significant, a higher percentage of C was found in the shoots in translocated plants compared to northern plants (Fig. 3b).

Similarly, the distribution of recently assimilated  $^{13}\text{C}$  among the plant and soil pools was uneven (Fig. 3d). In contrast to the partitioning pattern of total C within the plant pools, most of the  $^{13}\text{C}$  in both treatments was distributed to the leaves, followed by the shoot and the root. An insignificant increase in the percentage of  $^{13}\text{C}$  distributed to the shoot and the roots after translocation could be observed. Mineral soil contained a larger percentage distribution of  $^{13}\text{C}$  than the organic layer (Fig. 3d). Similar to the total C content of the plant, the amount of recently assimilated C also appeared to be influenced by

translocation. The total  $^{13}\text{C}$  mass recovered in the whole plant-soil system was higher in the translocated samples (Fig. 3c). In accordance, the  $\delta^{13}\text{C}$  (‰) in the leaves tended to increase by translocation (Table 3).

While the organic layer and mineral soil did only show a marginal accumulation of  $^{13}\text{C}$ , the MBC in the respective soil pools had higher  $\delta^{13}\text{C}$  values (Table 3). The share of the total assimilated  $^{13}\text{C}$  that was allocated to the microbial biomass was as high as the share for the respective soil fraction in total (Fig. 4). For both treatments, a higher percentage of assimilates was found in the organic layer. For both the organic layer and the mineral soil, translocation decreased the relative proportion of assimilates allocated to the microbial biomass. This effect was significant for the mineral soil, yet insignificant for the organic layer.

The total recovery in the soil and plant parts together with the tracer recovered in the  $\text{CO}_2$  efflux only sum up to  $725.17 \pm 90.99 \mu\text{g}$  and  $828.99 \pm 86.75 \mu\text{g } ^{13}\text{C}$ , representing 4.18% and 4.78% for northern and translocated samples, respectively (Table 2). Daily  $\text{CO}_2$  and  $^{13}\text{CO}_2$  measurements revealed that the percentage of  $^{13}\text{C}$  released as  $\text{CO}_2$  (relative to the total tracer recovered) was higher for northern control samples than translocated samples (Table 2). The  $^{13}\text{C}$  efflux decreased with time, while the  $\text{CO}_2$  efflux itself stayed constant (Fig. 5, Table 4). There was no effect of translocation on the daily  $\text{CO}_2$  efflux, but the cumulative efflux over eight days tended to decrease with translocation, yet not significantly. The  $\delta^{13}\text{C}$  of  $\text{CO}_2$  decreased more rapidly in translocated samples, leading to a higher decay constant  $k$  of the fitted exponential decay curve (Fig. 5).

The small-scale distribution of recently assimilated C in roots showed that root tips were more enriched in recently assimilated  $^{13}\text{C}$  than proximal root positions ( $p < 0.05$ , Fig. 6a). Root tips contained also clearly more  $^{13}\text{C}$  than the respective unlabelled control (Fig. 6b), demonstrating assimilation of the added  $^{13}\text{C}$  label. Although the enrichment of  $^{13}\text{C}$  in root tips was not significant in the unstained sample set, the results similarly revealed the tendency of higher enrichment at tips compared to proximal root positions (Fig. 6c). The colonization of root cells by ErM fungi, in contrast, had no effect on the  $\delta^{13}\text{C}$ , which becomes obvious when comparing infected cells with uninfected cells in the stained + labelled dataset (Fig. 6a).

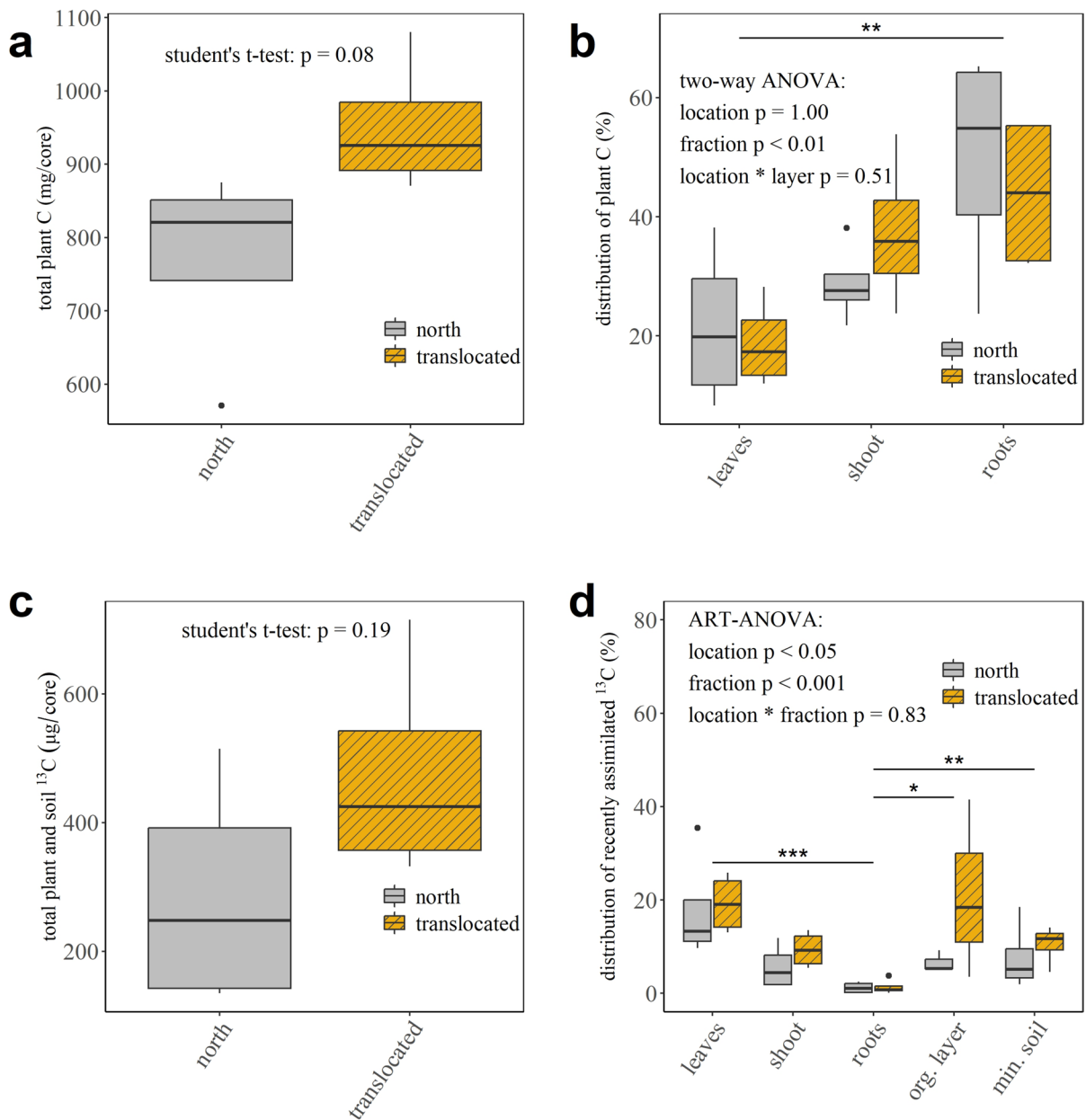


**Fig. 3** Carbon and  $^{13}\text{C}$  in *V. vitis-idaea*: The total Carbon in *V. vitis-idaea* (a) and its distribution in the plant pools (b). Total  $^{13}\text{C}$  recovered in the plant plus its associated soil after  $^{13}\text{CO}_2$ -pulse labelling (c) and its percentage distribution in the leaves, shoot, roots, organic layer (org.) and mineral soil (min., d). The percentage distribution of  $^{13}\text{C}$  is calculated relative to the total tracer recovered in the plant, soil, and  $\text{CO}_2$  efflux. The plants were translocated in intact cores together with its associated

soil from north to south Finland (+3.7 °C mean temperature, yellow, stripes) or translocated on site in north Finland (grey) and excavated after 2.5 years. Asterisks indicate significant differences between soil and plant fractions ( $p=0.05 < * < 0.01 < ** < 0.001 < ***$ ) tested with a two-way ANOVA or an aligned rank transformed (ART) two-way ANOVA followed by TukeyHSD or a post hoc test on estimated marginal means as respective post-hoc test ( $n=4$ )

**Table 2** Theoretical plant uptake of  $^{13}\text{C}$ , total tracer recovered, and  $^{13}\text{C}$  recovered in  $\text{CO}_2$  efflux: Table shows the added tracer per plant, the total tracer recovered in the plant-soil system and the  $\text{CO}_2$  efflux after eight days and the percentage of the total recovered  $^{13}\text{C}$  that was detected in the  $\text{CO}_2$  efflux.

|  | Northern control samples | Translocated samples<br>(+3.7 °C mean temperature) |
|--|--------------------------|--|
| Added tracer per plant (theoretical plant $^{13}\text{C}$ uptake)      | 17.35 mg                 |  |
| Total $^{13}\text{C}$ in soil–plant system and respiration             | 725.17 ± 90.99 µg        | 828.99 ± 86.75 µg                                  |
| Percentage of assimilated $^{13}\text{C}$ lost as $\text{CO}_2$ efflux | 63.3 ± 5.92%             | 44.1 ± 3.19%                                       |

**Table 3**  $\delta^{13}\text{C}$  of pools of the plant-soil system of *V. vitis-idaea*:  $\delta^{13}\text{C}$  values of different pools of the plant-soil system of *V. vitis-idaea* (average ± SE,  $n=4$ ) eight days after pulse labelling with  $^{13}\text{CO}_2$  and the respective natural abundance controls. Plants and the respective soil were either translocated

Plants and the respective soil were either translocated from North- to South-Finland (+3.7 °C mean temperature) or translocated on site in North-Finland as control. Values are presented as mean ± SE with  $n = 4$  except of the added tracer

from North- to South-Finland (+3.7 °C in mean temperature) or translocated on site in North-Finland as control. As natural abundance controls, additional plant and soil from North-Finland was used. An ANOVA revealed a significant effect of the compartment ( $p < 0.05$ )

| Compartment of the plant-soil system | Natural abundance $\delta^{13}\text{C}$ (‰) | $\delta^{13}\text{C}$ in northern controls (‰) | $\delta^{13}\text{C}$ in translocated samples (+3.7 °C mean temperature, ‰) |
|--------------------------------------|---|--|---|
| Leaves                               | -30.03 ± 1.06                               | 39.5 ± 9.0                                     | 57.7 ± 22.9   |
| Shoot                                | -29.68 ± 0.87                               | -11.5 ± 7.7                                    | -10.7 ± 4.5   |
| Roots                                | -29.38 ± 0.57                               | -25.6 ± 2.6                                    | -27.7 ± 0.9   |
| Rhizosphere                          | -28.28 ± 0.39                               | -27.9 ± 0.5                                    | -28.4 ± 0.2   |
| Mineral Soil                         | -28.13 ± 0.59                               | -26.5 ± 0.2                                    | -26.2 ± 0.3   |
| Organic Layer                        | -27.33 ± 0.61                               | -27.9 ± 0.1                                    | -27.27 ± 0.4  |
| MBC Mineral soil                     | -23.40 ± 2.30                               | 10.87 ± 13.69                                  | -24.91 ± 2.31   |
| MBC Organic layer                    | -32.60 ± 5.12                               | -19.38 ± 2.88                                  | -20.63 ± 2.09   |

## Discussion

### Patterns of total and recently assimilated C in the plant-soil system

In this study, we hypothesized that most of the overall biomass C and of the recently assimilated C are allocated to belowground pools. While the biomass C was mainly accumulated in the roots, followed by the shoot and the leaves, the recently assimilated C – traced as  $^{13}\text{C}$  after  $^{13}\text{CO}_2$ -pulse labelling – showed an inverse pattern. After eight days, leaves had the highest proportion of assimilated C (relative to the total  $^{13}\text{C}$  recovered in the plant and soil pools and the  $\text{CO}_2$  efflux), followed by the shoot and the roots (Fig. 3, Table 3), which is consistent with the findings of Kulmala et al. (2018). This disconnection of

overall C and recently assimilated C is a frequent occurrence (Kulmala et al. 2018; Litton et al. 2007). Although the short time of eight days after labelling in this study may have played a role in the distribution pattern, this phenomenon can also be attributed to temporal variations in C allocation patterns throughout the year (Saggar and Hedley 2001) and the life cycle of a plant (Kozłowski 1992). It has been observed that plants under nutrient limitation tend to allocate a significant amount of C into root biomass in the early live stages to access soil nutrients. When a sufficient root system is developed, plants subsequently shift the primary allocation to aboveground biomass, leading to the observed difference in allocation patterns (Kulmala et al. 2018).

While the highest C accumulation in roots compared to other plant parts in this study can be

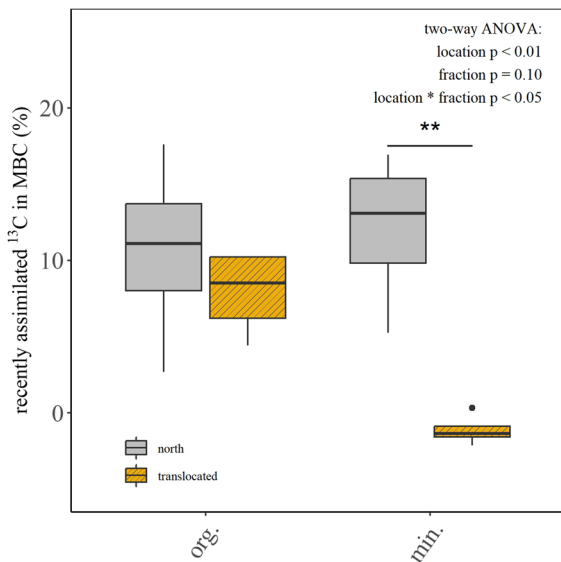


**Fig. 4**  $^{13}\text{C}$  in the microbial biomass in soil under *V. vitis-idaea*: Percentage of the total recovered assimilated C that was measured in the microbial biomass in the organic layer (org.) and the mineral soil (min.) of intact soil cores with *V. vitis-idaea*. Cores were either translocated from North to South-Finland (yellow, stripes, +3.7 °C mean temperature) or translocated on site in North-Finland as a control (grey). Stars indicate significant differences ( $p = 0.05 < * < 0.01 < ** < 0.01 < ***$ ) tested with a two-way ANOVA ( $n = 4$ ) and a TukeyHSD as a postdoc test

attributed to the high level of nutrient limitation typically observed in Podzols of boreal forests (Högberg et al. 2017; Olsrud and Christensen 2011), only a medium portion of the recently assimilated C is recovered in the roots and the soil. The highest portion of  $^{13}\text{C}$  was recovered in the  $\text{CO}_2$  efflux (Table 2). It cannot be differentiated between aboveground and belowground respiration in this study, but it was reported that around 20% of recent assimilates respired originate from belowground pools (Carbone and Trumbore 2007). We hypothesized that most of the overall biomass C and of the recently assimilated C are allocated in belowground pools. Our data only confirms the first part of this hypothesis, i.e. that most of the overall biomass C is allocated to belowground pools. Regarding the second part of the hypothesis, i.e. that also most of the recently assimilated C is allocated to belowground pools, we did not clearly find a high portion of recently assimilated C in root and soil. Similarly, in a  $^{13}\text{CO}_2$  labeling study, the  $^{13}\text{C}$

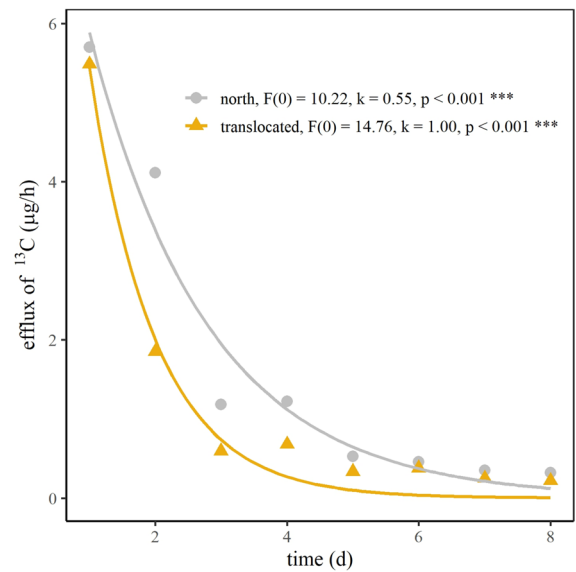


**Fig. 5** Exponential decay of  $^{13}\text{C}$  efflux from soil over an eight-day period following  $^{13}\text{C}$  pulse labelling. Symbols represent measured mean  $^{13}\text{C}$  efflux values for the *north* (grey circles) and *translocated* (yellow triangles) treatments. Lines show fitted exponential models  $F(t) = F_0 \cdot e^{-kt}$ , with decay constants of  $k = 0.55$  (*north*) and  $k = 1.00$  (*translocated*). Both fits were highly significant ( $p < 0.001$ )

enrichment of the rhizome was lower compared to the leaves and the shoot in *V. myrtillus* and *V. uliginosum* after eight days (Anadon-Rossel et al. 2017). This might indicate that the plants are not experiencing the expected need to invest their resources into nutrient acquisition at the phase of the study, potentially due to a yearly or lifetime rhythm of root development. This could also have implications for a seasonality in the contribution of boreal shrubs to forest C sequestration. After 8 days, most of the recently assimilated C was already respired, indicating that at least some of the respired C was previously allocated to the roots and soil. The high respiration of recently assimilated C generally matches results for *V. myrtillus* and *V. uliginosum*, but high interspecific variations in the speed of above- and below-ground metabolism is reported (Anadon-Rossel et al. 2017). Further partitioning of soil, root and shoot respiration needs to be conducted to confirm the belowground allocation of recent assimilates.

The percentage of the total assimilated C that was allocated to the soil microbial biomass was similar to the percentage we found to be allocated to

**Table 4** Carbon efflux and its  $\delta^{13}\text{C}$  from the plant-soil system of *V. vitis-idaea*: Carbon efflux and the respective  $\delta^{13}\text{C}$  of intact soil cores with *V. vitis-idaea* for up to 9 days after  $^{13}\text{CO}_2$ -pulse labelling (average  $\pm$  SE,  $n=4$ ) Cores were either translocated from North- to South-Finland ( $+3.7$  °C in mean

temperature) or translocated on site in North-Finland as control. A two-way ANOVA revealed no significant effect of day or location on C efflux. R values are given for the linear fit in the respective Miller/Tans plot. An asterix behind the  $R^2$  value indicates a significant fit ( $p < 0.05$ )

| Day after pulse labelling | Northern control samples |   |             | Translocated samples ( $+3.7$ °C mean temperature) |   |             |
|---------------------------|--------------------------|---|-------------|--|---|-------------|
|                           | C efflux (mg C/d)        | $\delta^{13}\text{C}$ in $\text{CO}_2$ efflux (‰) | $R^2$ value | C efflux (mg C/d)                                  | $\delta^{13}\text{C}$ in $\text{CO}_2$ efflux (‰) | $R^2$ value |
| 2                         | 20.5 $\pm$ 3.7           | 427.0 $\pm$ 203.2                                 | 0.47        | 27.5 $\pm$ 0.8                                     | 429.6 $\pm$ 332.8                                 | 0.22        |
| 3                         | 20.0 $\pm$ 3.9           | 417.0 $\pm$ 216.2                                 | 0.38        | 18.8 $\pm$ 2.9                                     | 122.4 $\pm$ 23.2                                  | 0.82 *      |
| 4                         | 18.4 $\pm$ 3.0           | 104.9 $\pm$ 41.3                                  | 0.52 *      | 25.6 $\pm$ 4.8                                     | 43.9 $\pm$ 9.3                                    | 0.79        |
| 5                         | 17.3 $\pm$ 3.8           | 120.8 $\pm$ 35.5                                  | 0.66 *      | 19.5 $\pm$ 0.6                                     | 32.8 $\pm$ 8.3                                    | 0.72        |
| 6                         | 17.1 $\pm$ 3.3           | 41.7 $\pm$ 14.6                                   | 0.58 *      | 19.6 $\pm$ 1.6                                     | 12.4 $\pm$ 9.6                                    | 0.22        |
| 7                         | 16.6 $\pm$ 3.7           | 33.1 $\pm$ 13.3                                   | 0.51 *      | 18.9 $\pm$ 1.1                                     | 16.8 $\pm$ 8.1                                    | 0.42        |
| 8                         | 15.0 $\pm$ 2.1           | 21.0 $\pm$ 17.8                                   | 0.19        | 18.9 $\pm$ 2.6                                     | 3.4 $\pm$ 2.6                                     | 0.22        |
| 9                         | 17.9 $\pm$ 2.3           | 13.9 $\pm$ 14.9                                   | 0.18        | 18.5 $\pm$ 1.3                                     | NA  | NA          |
| Cummulative               | 142.6 $\pm$ 18.6         |   |             | 167.3 $\pm$ 9.7                                    |   |             |

the soil (Fig. 4). In other words, nearly all recently assimilated C that was exudated into the soil within 8 days was either incorporated into the microbial biomass or already respired. This finding is in line with the results of Olsrud and Christensen (2011), who showed that MBC represents the largest belowground pool of recently assimilated C following in-situ  $^{14}\text{C}$  pulse-labelling. The distribution of assimilated C towards soil microbes of *V. vitis-idaea* as part of our hypothesis (I) can be confirmed and suggests a tight relationship between plant and symbiotic soil microorganisms in nutrient limiting conditions.

When comparing the total  $^{13}\text{C}$  recovered in the plant and soil compartments and the  $\text{CO}_2$  efflux with the amount of  $^{13}\text{C}$  tracer addition (one plant could have theoretically assimilated 17 mg per plant), we only recovered below 5 %. This suggests that most of the added  $^{13}\text{CO}_2$  was not taken up by photosynthetic activity of *V. vitis-idaea*. In an in-situ labelling study of peatland shrubs, the total recovery of  $^{13}\text{C}$  was around 25% (Zeh et al. 2022). In the present study, however, more tracer (2 g compared to 0.6 g  $\text{Na}_2^{13}\text{CO}_3$ ) was applied to ensure the recovery of sufficient label in plant and soil pools. Nevertheless, it also needs to be considered that the uptake of tracer could be underestimated as the study could miss a relevant pool: Respiration of  $^{13}\text{CO}_2$  was not measured on the first day after labeling, and the C allocation to flowers, which formed during the eight days after labelling, were not taken into account.

#### Distribution of recently assimilated C in ErM infected fine roots

We hypothesized that recently assimilated C is transferred preferentially to root tips and that those root parts are therefore highly enriched in  $^{13}\text{C}$  when compared to other root parts (hypothesis II). Here, we investigated the distribution of  $^{13}\text{C}$  within fine roots and found, indeed, that only tips contained more  $^{13}\text{C}$  than the unlabelled control and were therefore enriched in recently assimilated C (Fig. 6). A preferential transport of recently assimilated C into root tips was also observed by Pausch and Kuzyakov (2011). Yet, the enrichment in root tips was still low in comparison with leaves or stems, which can be attributed, again, to small C allocation to the root system at that stage of growing season and life cycle (Ding et al. 2020). Furthermore, Pausch and Kuzyakov (2011) observed that hotspots located at root tips persisted for at least two days but not more than eleven days. Following this finding, the rather small enrichment of root tips in our approach, i.e. eight days after pulse-labelling, might alternatively indicate a fast turnover of roots with replacement of  $^{13}\text{C}$  by subsequent unlabelled C.

We further hypothesized that a larger proportion of recently assimilated C is transferred to root cells colonized by mycorrhizal fungi (Fig. 6). This could be assumed as plants invest into nutrient acquisition strategies in such nutrient poor soils. However, this hypothesis could not be confirmed and we found no

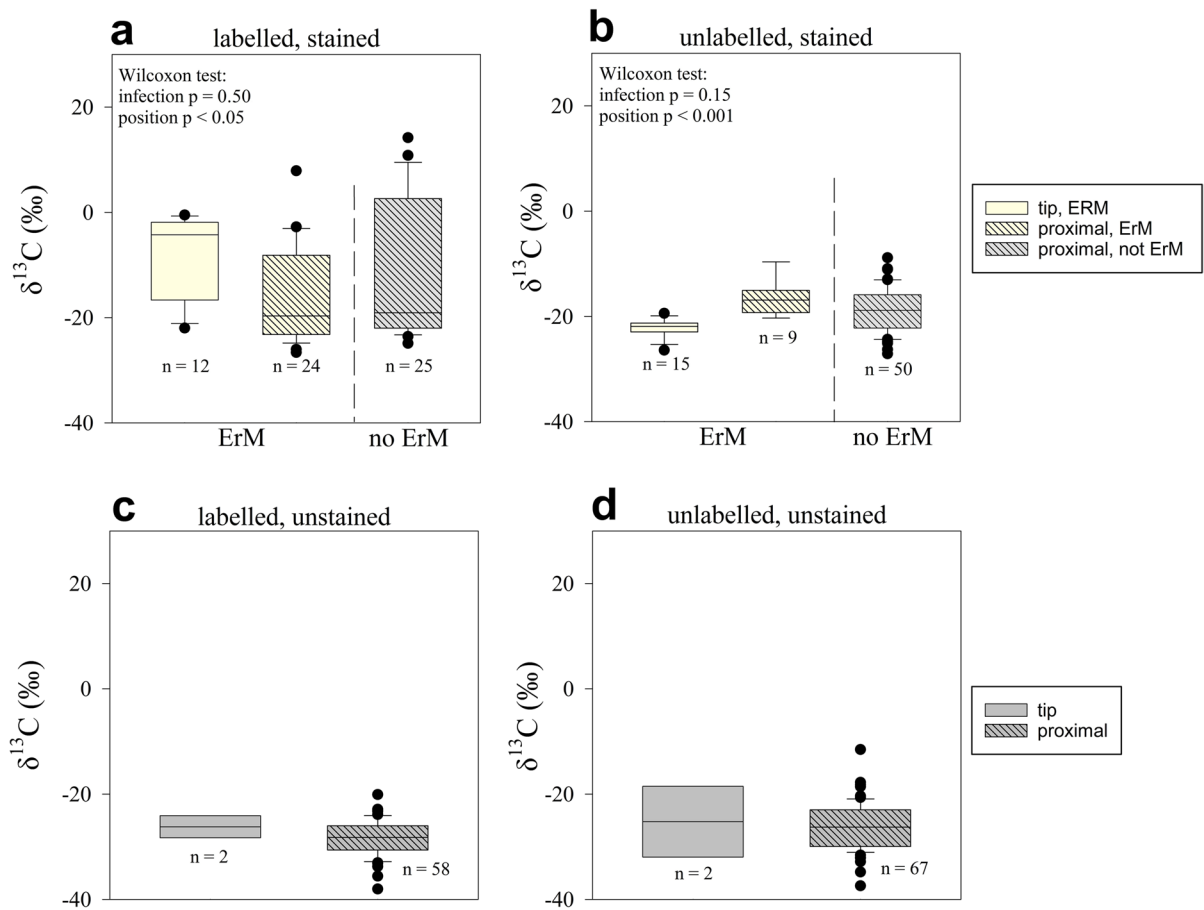


**Fig. 6**  $\delta^{13}\text{C}$  in fine roots of *Vaccinium vitis-idaea*:  $\delta^{13}\text{C}$  in parts of the fine roots of *Vaccinium vitis-idaea*, that were pulse labelled with  $^{13}\text{CO}_2$  (a, c) and stained with trypan blue to make ErM colonization visible (a, b) and the respective controls (d).

difference in  $^{13}\text{C}$  assimilation between ErM colonized and non-colonized cells. This could indicate that recently assimilated C is not preferentially transferred to ErM colonized cells under these conditions or as discussed above, rapidly replaced with unlabelled C.

#### Effect of warming on C allocation in *V. vitis-idaea*

Besides identifying the general C allocation patterns of *V. vitis-idaea*, the objective of this study was to analyze their changes in response to a short-term warming (i.e. 2.5 years) that was simulated by a translocation approach from North to South Finland. As SOM decomposition is expected to increase with rising temperatures (Wang et al. 2018), potentially leading to a higher nutrient availability under warming (Bai et al.

Fine root parts with a visible ErM colonization are displayed in yellow and parts with no visible colonization or an unknown colonization status are displayed in grey. Proximal root parts are displayed with grey stripes

2013; Schmidt et al. 2002), we hypothesized a shift in C allocation, leading to reduced C transfer to roots, soil, and microbial biomass. The translocation, however, seemed to have only minor effects and mainly trends but no significant effect could be observed. We observed a tendency of stimulated plant growth, which was indicated by a higher total plant biomass and, therefore, a higher plant C stock. In line with that, higher  $^{13}\text{C}$  uptake by translocated plants was observed, as more  $^{13}\text{C}$  was recovered in translocated cores when combining plant, soil, and  $\text{CO}_2$  efflux (Fig. 3). This could indicate a higher photosynthetic activity of the translocated plants and may be associated with warming-induced increases in the photosynthetic process itself (Reich et al. 2018) and with the better growth of translocated plants, which produced more biomass capable

to perform photosynthesis. Higher accumulation of C in the shoot as well as a higher proportion of recently assimilated C in aboveground plant parts after translocation, however, could indicate a lower need of plants to invest into roots due to a higher nutrient availability in the soil (Bonifas et al. 2005). The latter might result from higher SOM decomposition rates in warmer soils (Klimek et al. 2020), as proposed in hypothesis (III). This interpretation is based on the assumption that the C allocation pattern eight days after labelling is representative for warming-induced differences in C allocation. We are aware that  $^{13}\text{C}$  may continue to accumulate in roots within the subsequent days (Zhou et al. 2022) and we cannot exclude that differences between treatments would have been differently expressed at later stages. Yet, seven days after labelling has been shown to be the time when C allocation to roots is maximal (Zhou et al. 2022). Concluding, while the translocation had only minor effects on soil C and N, a tendency towards higher plant C stock suggests a warming induced increased enzymatic activity. Further, a greater allocation of C towards plant shoot suggests a change in plant nutrient acquisition. This could imply that under warming, less C is allocated in belowground parts by *V. vitis-idaea*, potentially decreasing their contribution to the soil C sequestration in boreal forests.

The  $^{13}\text{C}$  efflux of the translocated samples decreased more rapidly compared to the northern samples (Fig. 5, Table 4), which implies a faster turnover of C in the translocated samples. This could indicate a higher microbial activity. Higher microbial activities due to warming were frequently reported (Xu et al. 2023) and are also supported by higher overall respiration of the translocated samples compared to the northern samples (Table 4). A higher microbial activity can lead to faster nutrient mineralization in the soil (Melillo et al. 2002) supporting the explanation given for the greater C allocation towards the shoot. Compared to the northern control samples, a smaller percentage of the assimilated  $^{13}\text{C}$  was recovered in the respiration (Table 2). However, due to the sharper decrease in  $^{13}\text{C}$  efflux of translocated samples, we can expect that on the first day, where no gas measurement was conducted, more  $^{13}\text{C}$  was released in translocated samples compared to northern controls. This can serve as an explanation for the lower percentage of assimilated  $^{13}\text{C}$  distributed to the cumulative  $\text{CO}_2$  efflux from translocated samples.

Apart from a tendency towards higher invest of C into the plant shoot and leaves, recovery patterns in the plant-soil system remained mostly unchanged (Fig. 3). Similarly, the  $\delta^{13}\text{C}$  values in the rhizosphere remained unaffected by translocation (Table 3). Therefore, we cannot fully support our hypothesis (III) that a faster soil nutrient mineralization induced by translocation would result in a shift in plant C distribution patterns. It is possible that the chosen time of 2.5 years of translocation was not enough to detect such profound changes in the C distribution patterns. In general, it may also be that the distribution of new, recently assimilated C within the plant-soil system exhibits a high degree of plasticity and was influenced by the exposure to the temperature-controlled climate chamber. Thus, a potential role of short-term adaptation to the conditions in the climate chamber must be kept in mind when interpreting the results.

We further expected as part of hypothesis (III) that less photosynthetically assimilated C can be found in the microbial biomass after translocation. The  $^{13}\text{C}$  signal was indeed lower in the MBC in the mineral soil after translocation (Fig. 4, Table 3). This observation could be explained in two contrasting mechanisms: In line with our hypothesis, a higher microbial decomposition and an associated higher nutrient availability after translocation could lead to less plant need to invest assimilates to soil microorganisms, such as ErM fungi, for nutrient acquisition. This is also supported by findings from a study conducted with the *Ericaceous* shrub *R. nigrum* ssp. *hermaphroditum* (Hupperts et al. 2024), where less dependence of the shrub on the mycorrhizal partner under warming was shown and a higher mineralization was indicated using isotope labelling. However, this seems to be dependent on the recalcitrance of the nutrient source (Hupperts et al. 2024). However, on the other hand, the general faster cycling of  $^{13}\text{C}$  in translocated samples in our study (e.g. indicated by a faster decrease in  $^{13}\text{CO}_2$ ) could imply that less  $^{13}\text{C}$  was retained in the microbial biomass and it was instead already released as  $\text{CO}_2$  again. Which mechanism explains the observed finding better remains to be elucidated. Nevertheless, this part of hypothesis (III) can be cautiously accepted as translocation led to less  $^{13}\text{C}$  in soil microorganisms.

## Conclusion

In summary, the findings of this study highlight that C allocation into the root system of *V. vitis-idaea* is only marginally affected by 2.5 years of warming. Most of the results, however, suggest an increase in the soil microbial activity and higher SOM mineralization under global warming. This may lead to more profound changes in plant properties and allocation over longer time spans than studied here. Especially, this may lead to less plant investment into ErM fungal partners which could have – together with the higher mineralization rate – important implications for C sequestration in boreal forests. To verify these interpretations, future studies need to be conducted to further analyze the importance of ErM symbioses under global warming.

## Appendix

Figure 7.



**Fig. 7** Example of a small-scale  $^{13}\text{C}$  measurement using LA-IRMS after root staining to visualize ErM colonized root parts

**Acknowledgements** This research was supported by funds from the Helsinki Institute of Life Science (a HiLIFE Fellow grant to KK), Academy of Finland (Grant numbers 319952 & 316401, 348824), Maj and Tor Nessling foundation (personal grant to O-MS), and the DFG (German Research Foundation, priority program 2089 “Rhizosphere spatiotemporal organization – a key to rhizosphere function”, project number 403670844). The authors would like to thank BayCenSI (Bayreuth Center for stable Isotope research) for isotope analyses and CAN (Center for chemical analysis) Bayreuth for C and N analyses. Further, the authors would like to thank the technical assistance of Karin Söllner, Lisa Rohn for creating the map presented in the manuscript, and Jana Kehr for assistance in the laboratory. Dr. Päivi Merilä is gratefully acknowledged for facilitating the establishment of the translocation experiment.

**Author contributions** VBK: conceptualization, data curation, investigation, formal analysis, investigation, writing—original draft, writing – review & editing, visualization O-MS: conceptualization, funding acquisition, project administration, writing – review & editing, KK: conceptualization, funding acquisition, writing – review & editing, AR: data curation, formal analysis, investigation, writing – review & editing, ST: methodology, writing – review & editing, TO: investigation, formal analysis, writing – review & editing, EL: funding acquisition, conceptualization, writing – review & editing, JP: formal analysis, data curation, supervision, writing—original draft, writing – review & editing, NM: project administration, supervision, conceptualisation, writing—original draft, writing – review & editing.

**Funding** Open Access funding enabled and organized by Projekt DEAL.

**Data availability** The dataset generated and analysed during the current study are available from the corresponding author on request.

## Declarations

**Competing interests** All authors certify that they have no affiliations with or involvement in any organization or entity with any financial interest or non-financial interest in the subject matter or materials discussed in this manuscript.

**Open Access** This article is licensed under a Creative Commons Attribution 4.0 International License, which permits use, sharing, adaptation, distribution and reproduction in any medium or format, as long as you give appropriate credit to the original author(s) and the source, provide a link to the Creative Commons licence, and indicate if changes were made. The images or other third party material in this article are included in the article’s Creative Commons licence, unless indicated otherwise in a credit line to the material. If material is not included in the article’s Creative Commons licence and your intended use is not permitted by statutory regulation or exceeds the permitted use, you will need to obtain permission directly

from the copyright holder. To view a copy of this licence, visit <http://creativecommons.org/licenses/by/4.0/>.

## References

- Anadon-Rossel A, Hasibeder R, Palacio S, Mayr S, Ingrisich J, Ninot JM, Nogués S, Bahn M (2017) Short-term carbon allocation dynamics in subalpine dwarf shrubs and their responses to experimental summer drought. *Environ Exp Bot* 141:92–102. <https://doi.org/10.1016/j.envexpbot.2017.07.006>
- Backhaus S, Kreyling J, Beierkuhnlein C, Buhk C, Nagy L, Thiel D, Jentsch A (2014) A transplantation experiment along climatic gradients suggests limitations of experimental warming manipulations. *Clim Res* 60(1):63–71. <https://doi.org/10.3354/cr01219>
- Bai E, Li S, Xu W, Li W, Dai W, Jiang P (2013) A meta-analysis of experimental warming effects on terrestrial nitrogen pools and dynamics. *New Phytol* 199(2):441–451. <https://doi.org/10.1111/nph.12252>
- Bekku YS, Nakatsubo T, Kume A, Adachi M, Koizumi H (2003) Effect of warming on the temperature dependence of soil respiration rate in arctic, temperate and tropical soils. *Appl Soil Ecol* 22(3):205–210. [https://doi.org/10.1016/S0929-1393\(02\)00158-0](https://doi.org/10.1016/S0929-1393(02)00158-0)
- Bergeron O, Margolis HA, Coursolle C (2009) Forest floor carbon exchange of a boreal black spruce forest in eastern North America. *Biogeosciences* 6(9):1849–1864. <https://doi.org/10.5194/bg-6-1849-2009>
- Bonifas KD, Walters DT, Cassman KG, Lindquist JL (2005) Nitrogen supply affects root: shoot ratio in corn and velvetleaf (*Abutilon theophrasti*). *Weed Sci* 53(5):670–675. <https://doi.org/10.1614/WS-05-002R.1>
- Bradshaw CJA, Warkentin IG (2015) Global estimates of boreal forest carbon stocks and flux. *Glob Planet Change* 128:24–30. <https://doi.org/10.1016/j.gloplacha.2015.02.004>
- Carbone MS, Trumbore SE (2007) Contribution of new photosynthetic assimilates to respiration by perennial grasses and shrubs: residence times and allocation patterns. *New Phytol* 176(1):124–135. <https://doi.org/10.1111/j.1469-8137.2007.02153.x>
- Clemmensen KE, Finlay RD, Dahlberg A, Stenlid J, Wardle DA, Lindahl BD (2015) Carbon sequestration is related to mycorrhizal fungal community shifts during long-term succession in boreal forests. *New Phytol* 205(4):1525–1536. <https://doi.org/10.1111/nph.13208>
- Coetzee BWT, van Zyl L (2024) The environmental light characteristics of forest under different logging regimes. *Ecol Evol* 14:e70623. <https://doi.org/10.1002/ece3.70623>
- Dawes MA, Hagedorn F, Zumbunn T, Handa IT, Hättenschwiler S, Wipf S, Rixen C (2011) Growth and community responses of alpine dwarf shrubs to in situ CO<sub>2</sub> enrichment and soil warming. *New Phytol* 191(3):806–818. <https://doi.org/10.1111/j.1469-8137.2011.03722.x>
- Ding Y, Leppälampi-Kujansuu J, Helmisaari H-S (2019) Fine root longevity and below- and aboveground litter production in a boreal *Betula pendula* forest. *Forest Ecol Manag* 431:17–25. <https://doi.org/10.1016/j.foreco.2018.02.039>
- Ding Y, Schiestl-Aalto P, Helmisaari H-S, Makita N, Ryhti K, Kulmala L (2020) Temperature and moisture dependence of daily growth of Scots pine (*Pinus sylvestris* L.) roots in Southern Finland. *Tree Physiol* 40(2):272–283. <https://doi.org/10.1093/treephys/tpz131>
- FC M, Davis TL, Wickham H (2025) ggpattern: ‘ggplot2’ Pattern Geoms. <https://github.com/trevorld/ggpattern>
- Finnish Meteorological Institute (2025) Observational dataset. Retrieved from <https://en.ilmatieteenlaitos.fi/download-observations> on 12.08.2025
- Forkel M, Carvalhais N, Rödenbeck C, Keeling R, Heimann M, Thonicke K, Zaehle S, Reichstein M (2016) Enhanced seasonal CO<sub>2</sub> exchange caused by amplified plant productivity in northern ecosystems. *Science* 351(6274):696–699. <https://doi.org/10.1126/science.aac4971>
- Fox J, Sanford W, Daniel A, Douglas B, Gabriel B-B, Steve E, David F (2012) "Package ‘car.’" Vienna: R Foundation for Statistical Computing 16(332):333
- Gavrichkova O, Liberati D, Gunina A, Guidolotti G, de Dato G, Calfapietra C, de Angelis P, Brugnoli E, Kuzyakov Y (2017) Does long-term warming affect C and N allocation in a Mediterranean shrubland ecosystem? Evidence from a <sup>13</sup>C and <sup>15</sup>N labeling field study. *Environ Exp Bot* 141:170–180
- Hawkins H-J, Cargill RIM, van Nuland ME, Hagen SC, Field KJ, Sheldrake M, Suodzilovskaia NA, Kiers ET (2023) Mycorrhizal mycelium as a global carbon pool. *Curr Biol* 33(11):R560–R573. <https://doi.org/10.1016/j.cub.2023.02.027>
- Högberg P, Näsholm T, Franklin O, Högberg MN (2017) Tamm review: on the nature of the nitrogen limitation to plant growth in Fennoscandian boreal forests. *For Ecol Manag* 403:161–185. <https://doi.org/10.1016/j.foreco.2017.04.045>
- Hupperts SF, Islam KS, Gundale MJ, Kardol P, Sundqvist MK (2024) Warming influences carbon and nitrogen assimilation between a widespread *Ericaceous* shrub and root-associated fungi. *New Phytol* 241(3):1062–1073. <https://doi.org/10.1111/nph.19384>
- Ilvesniemi H, Levula J, Ojansuu R, Kolari P, Kulmala L, Pumpanen J, Launiainen S, Vesala T, Nikinmaa E (2009) Long-term measurements of the carbon balance of a boreal Scots pine dominated forest ecosystem. *Boreal Environ Res* 14:731–753
- Jenkinson DS, Brookes PC, Powlson DS (2004) Measuring soil microbial biomass. *Soil Biol Biochem* 36(1):5–7. <https://doi.org/10.1016/j.soilbio.2003.10.002>
- Kay M, Elkin L, Higgins J, Wobbrock J (2025) ARTool: Aligned Rank Transform for Nonparametric Factorial ANOVAs. <https://doi.org/10.5281/zenodo.594511>
- Klimek B, Chodak M, Jaźwa M, Azarbad H, Niklińska M (2020) Soil physicochemical and microbial drivers of temperature sensitivity of soil organic matter decomposition under boreal forests. *Pedosphere* 30(4):528–534. [https://doi.org/10.1016/S1002-0160\(17\)60400-4](https://doi.org/10.1016/S1002-0160(17)60400-4)
- Kolari P, Pumpanen J, Kulmala L, Ilvesniemi H, Nikinmaa H, Grönholm T, Hari P (2006) Forest floor vegetation plays an important role in photosynthetic production of boreal forests. *Forest Ecol Manag* 221(1–3):241–248. <https://doi.org/10.1016/j.foreco.2005.10.021>

- Kozłowski TT (1992) Carbohydrate sources and sinks in woody plants. *Bot Rev* 58(2):107–222. <https://doi.org/10.1007/BF02858600>
- Kulmala L, Pumpanen J, Kolari P, Muukkonen P, Hari P, Vesala T (2011) Photosynthetic production of ground vegetation in different-aged Scots pine (*Pinus sylvestris*) forests. *Can J for Res* 41(10):2020–2030. <https://doi.org/10.1139/x11-121>
- Kulmala L, del Rosario Dominguez Carrasco M, Heinonsalo J (2018) The differences in carbon dynamics between boreal dwarf shrubs and Scots pine seedlings in a microcosm study. *J Plant Ecol* 11(5):709–716. <https://doi.org/10.1093/jpe/rtx051>
- Kuzyakov Y (2001) Tracer studies of carbon translocation by plants from the atmosphere into the soil (a review). *Eurasian Soil Sci* 34(1):28–42
- Lenth R, Piaskowski J (2025) emmeans: Estimated Marginal Means, aka Least-Squares Means. R package version 2.0.0. <https://rvlenth.github.io/emmeans/>
- Litton CM, Raich JW, Ryan MG (2007) Carbon allocation in forest ecosystems. *Glob Change Biol* 13(10):2089–2109. <https://doi.org/10.1111/j.1365-2486.2007.01420.x>
- Lupi C, Morin H, Deslauriers A, Rossi S, Houle D (2013) Role of soil nitrogen for the conifers of the Boreal Forest: a critical review. *Int J Plant Sci* 2(2):155–189. <https://doi.org/10.9734/IJPS/2013/4233>
- Melillo JM, Steudler PA, Aber JD, Newkirk K, Lux H, Bowles FP, Catricala C, Magill A, Ahrens T, Morrisseau S (2002) Soil warming and carbon-cycle feedbacks to the climate system. *Science* 298(5601):2173–2176. <https://doi.org/10.1126/science.1074153>
- Merilä P, Lindroos AJ, Helmisaari HS, Hilli S, Nieminen TM, Nöjd P, Rautio P, Salemaa M, Tupek B, Ukonmaanaho L (2024) Carbon stocks and transfers in coniferous boreal forests along a latitudinal gradient. *Ecosystems* 27:151–167. <https://doi.org/10.1007/s10021-023-00879-5>
- Merilä P, Mustajärvi K, Helmisaari HS, Hilli S, Lindroos AJ, Nieminen TM, Nöjd P, Rautio P, Salemaa M, Ukonmaanaho L (2014) Above- and below-ground N stocks in coniferous boreal forests in Finland: implications for sustainability of more intensive biomass utilization. *For Ecol Manag* 311:17–28. <https://doi.org/10.1016/j.foreco.2013.06.029>
- Mielke LA, Ekblad A, Finlay RD, Fransson P, Lindahl BD, Clemmensen KE (2022) Ericaceous dwarf shrubs contribute a significant but drought-sensitive fraction of soil respiration in a boreal pine forest. *J Ecol* 110(8):1928–1941. <https://doi.org/10.1111/1365-2745.13927>
- Miller JB, Tans PP (2003) Calculating isotopic fractionation from atmospheric measurements at various scales. *Tellus B* 55(2):207. <https://doi.org/10.3402/tellusb.v55i2.16697>
- Murage EW, Voroney PR (2007) Modification of the original chloroform fumigation extraction technique to allow measurement of  $\delta^{13}\text{C}$  of soil microbial biomass carbon. *Soil Biol Biochem* 39(7):1724–1729. <https://doi.org/10.1016/j.soilbio.2007.01.026>
- Ohlsson KEA (2013) Uncertainty of blank correction in isotope ratio measurement. *Anal Chem* 85(11):5326–5329. <https://doi.org/10.1021/ac4003968>
- Olsrud M, Christensen TR (2011) Carbon partitioning in a wet and a semiwet subarctic mire ecosystem based on in situ  $^{14}\text{C}$  pulse-labelling. *Soil Biol Biochem* 43(2):231–239. <https://doi.org/10.1016/j.soilbio.2010.09.034>
- Pausch J, Kuzyakov Y (2011) Photoassimilate allocation and dynamics of hotspots in roots visualized by  $^{14}\text{C}$  phosphor imaging. In *z Pflanzenernähr Boden* 174(1):12–19. <https://doi.org/10.1002/jpln.200900271>
- R Core Team (2023): R: A Language and Environment for Statistical Computing. R Foundation for Statistical Computing, Vienna, Austria
- Reich PB, Sendall KM, Stefanski A, Rich RL, Hobbie SE, Montgomery RA (2018) Effects of climate warming on photosynthesis in boreal tree species depend on soil moisture. *Nature* 562(7726):263–267. <https://doi.org/10.1038/s41586-018-0582-4>
- Rodionov A, Lehndorff E, Stremtan CC, Brand WA, Königshoven H-P, Amelung W (2019) Spatial microanalysis of natural  $^{13}\text{C}/^{12}\text{C}$  abundance in environmental samples using laser ablation-isotope ratio mass spectrometry. In *Anal Chem* 91(9):6225–6232. <https://doi.org/10.1021/acs.analchem.9b00892>
- Ruosteenoja K, Jylhä K (2021) Projected climate change in Finland during the 21<sup>st</sup> century calculated from CMIP6 model simulations. *Geophysica* 65(1):39–69
- Saggarr S, Hedley CB (2001) Estimating seasonal and annual carbon inputs, and root decomposition rates in a temperate pasture following field  $^{14}\text{C}$  pulse-labelling. *Plant Soil* 236(1):91–103. <https://doi.org/10.1023/A:1011942619252>
- Schmidt IK, Jonasson S, Shaver GR, Michelsen A, Nordin A (2002) Mineralization and distribution of nutrients in plants and microbes in four arctic ecosystems: responses to warming. *Plant Soil* 242(1):93–106. <https://doi.org/10.1023/A:1019642007929>
- Sietiö O-M, Tuomivirta T, Santalahti M, Kiheri H, Timonen S, Sun H, Fritze H, Heinonsalo J (2018) Ericoid plant species and *Pinus sylvestris* shape fungal communities in their roots and surrounding soil Summary. *New Phytol* 218(2):738–751. <https://doi.org/10.1111/nph.15040>
- Smith SE, Read DJ (2010) Mycorrhizal symbiosis. Academic press, London, UK
- Swanson RV, Flanagan LB (2001) Environmental regulation of carbon dioxide exchange at the forest floor in a boreal black spruce ecosystem. *Agric for Meteorol* 108(3):165–181
- van der Heijden MGA, Bardgett RD, van Straalen NM (2008) The unseen majority: soil microbes as drivers of plant diversity and productivity in terrestrial ecosystems. *Ecol Lett* 11(3):296–310. <https://doi.org/10.1111/j.1461-0248.2007.01139.x>
- Vance ED, Brookes PC, Jenkinson DS (1987) An extraction method for measuring soil microbial biomass C *Soil Biology and Biochemistry* 19(6):703–707. [https://doi.org/10.1016/0038-0717\(87\)90052-6](https://doi.org/10.1016/0038-0717(87)90052-6)
- Vergara Sosa M, Lehndorff E, Rodionov A, Gocke M, Sandhage-Hofmann A, Amelung W (2021) Micro-scale resolution of carbon turnover in soil - Insights from laser ablation isotope ratio mass spectrometry on water-glass embedded aggregates. *Soil Biol Biochem* 159:108279. <https://doi.org/10.1016/j.soilbio.2021.108279>
- Wang Q, Zhao X, Chen L, Yang Q, Chen S, Zhang W (2018) Global synthesis of temperature sensitivity of soil organic

- carbon decomposition: Latitudinal patterns and mechanisms. *Fun Ecol* 33(3):514–523. <https://doi.org/10.1111/1365-2435.13256>
- Ward EB, Duguid MC, Kuebbing SE, Lendemer JC, Bradford MA (2022) The functional role of ericoid mycorrhizal plants and fungi on carbon and nitrogen dynamics in forests. *New Phytol* 235(5):1701–1718. <https://doi.org/10.1111/nph.18307>
- Warembourg, F.R., Estelrich, D.H., and Lafont, F., Carbon Partitioning in the Rhizosphere of an Annual and a Perennial Species of Bromegrass, *Symbiosis*, 1990, vol. 9, pp. 29–36.
- Werner RA, Brand WA (2001) Referencing strategies and techniques in stable isotope ratio analysis. *Rapid Commun Mass Spectrom* 15(7):501–519. <https://doi.org/10.1002/rcm.258>
- Werner RA, Bruch BA, Brand WA (1999) ConFlo III - an interface for high precision  $\delta^{13}\text{C}$  and  $\delta^{15}\text{N}$  analysis with an extended dynamic range. *Rapid Commun. Mass Spectrom* 13(13):1237–1241. [10.1002/\(SICI\)1097-0231\(19990715\)13:13<1237::AID-RCM633>3.0.CO;2-C](https://doi.org/10.1002/(SICI)1097-0231(19990715)13:13<1237::AID-RCM633>3.0.CO;2-C)
- Wickham H (2016) *ggplot2: Elegant Graphics for Data Analysis*. Springer-Verlag, New York, USA
- Wilke CO (2024) cowplot: Streamlined Plot Theme and Plot Annotations for 'ggplot2', <https://wilkelab.org/cowplot/>
- Wobbrock J, Findlater L, Gergle D, Higgins J (2011) The Aligned Rank Transform for Nonparametric Factorial Analyses Using Only ANOVA Procedures. *Proc ACM CHI '11*. 134–146. <https://doi.org/10.1145/1978942.1978963>
- Xu H, Huang L, Chen J, Zhou H, Wan Y, Qu Q, Miggang W, Sha X (2023) Changes in soil microbial activity and their linkages with soil carbon under global warming. *CATENA* 232:107419. <https://doi.org/10.1016/j.catena.2023.107419>
- Yun H, Ciais P, Zhu Q, Chen D, Zohner CM, Tang J, Qu Y, Zhou H, Schimel J, Zhu P, Shao M, Christensen JH, Wu Q, Chen A, Eberling B (2024) Changes in above- versus belowground biomass distribution in permafrost regions in response to climate warming. *PNAS* 121(25):e2314036121. <https://doi.org/10.1073/pnas.2314036121>
- Zeh L, Schmidt-Cotta C, Limpens J, Bragazza L, Kalbitz K (2022) Above-to belowground carbon allocation in peatlands shifts with plant functional type and temperature. *J Plant Nutr Soil Sci* 185:98–109. <https://doi.org/10.1002/jpln.202100206>
- Zhou J, Shao G, Kumar A, Shi L, Kuzyakov Y, Pausch J (2022) Carbon fluxes within tree-crop-grass agroforestry system:  $^{13}\text{C}$  field labeling and tracing. *Biol Fertil Soils* 58(7):733–743. <https://doi.org/10.1007/s00374-022-01659-4>

**Publisher's Note** Springer Nature remains neutral with regard to jurisdictional claims in published maps and institutional affiliations.